Received: 10 May 2019 | Revised: 19 September 2019 | Accepted: 23 October 2019

DOI: 10.1002/bio.3735

RESEARCH ARTICLE

LUMINESCENCE The Journal of Biological and Chemical Luminescence WILEY

Luminescence properties of the Ln–EDTA complexes covalently linked to the chitosan biopolymers containing β-diketonate as antenna ligands

Israel F. Costa[1] | Gilvan P. Pires[1] | José Geraldo P. Espínola[1] | Hermi F. Brito[2] | Maria Claudia F.C. Felinto[3] | Wagner M. Faustino[1] | Ercules E.S. Teotonio[1]

[1]Departamento de Química, Universidade Federal da Paraíba, João Pessoa, PB, Brazil

[2]Departamento de Química Fundamental, Instituto de Química da Universidade de São Paulo, São Paulo, SP, Brazil

[3]Instituto de Pesquisas Energéticas e Nucleares, Travessa R 400 Cidade Universitária, São Paulo, SP, Brazil

Correspondence
Ercules E. S. Teotonio, Departamento de Química – Universidade Federal da Paraíba, 58051-900. João Pessoa – PB, Brazil.
Email: teotonioees@quimica.ufpb.br

Funding information
Conselho Nacional de Desenvolvimento Científico e Tecnológico, Grant/Award Number: Process number: 508889/2010-3

Abstract

This paper reports on the preparation, characterization, and photoluminescence properties of novel hybrid materials, in which the EDTA–Ln–L complexes (where L: H_2O, acac, bzac, dbm, and tta ligands, and Ln: Eu, Gd, and Tb) were covalently linked to the precursor medium molecular weight chitosan surface (CS) matrices or on the chitosan surfaces previously crosslinked with epichlorohydrin (CSech). The emission spectra of these materials were characterized by intraconfigurational-4fN transitions centred on the Eu^{3+} and Tb^{3+} ions. Some broad bands from the polymeric matrix were also observed in the emission spectra, however the relative intensities of the intraconfigurational bands increased significantly for systems containing diketonate ligands when the antenna effect became more efficient. The values of the radiative rates (A_{rad}) were higher for crosslinked hybrid systems with epichlorohydrin, while nonradiative rates (A_{nrad}) presented the opposite behaviour. These data contributed to an increase in the values of emission quantum efficiency (η) for crosslinked materials. The effect of the modification process and antenna ligand on the values of intensities, intensity parameters Ω_2 e Ω_4 of the Eu^{3+} complexes were also investigated. The results showed that the crosslinked biopolymer surfaces have great potential for applications in molecular devices light converters.

1 | INTRODUCTION

Chitosan represents one of the most explored biopolymers, finding innovative industrial applications in different fields ranging from textile and paper industries to pharmacy and agriculture.[1–3] In the areas of basic research, these materials have gained growing importance for the development of new, advanced, and multifunctional systems with potential for applications as sensors[4,5], catalysts[6,7], and luminescent markers.[8,9] The main driving forces behind the interest in chitosan-based materials include the demand for functional systems exhibiting new marked properties, cost–effectiveness, biocompatibility, and intrinsic structural features due to the presence of acetylamido, hydroxyl, and amine functional groups.[10,11] It is noteworthy that these groups can be covalently modified by different, synergistically coupled organic molecules to obtain a wide range of materials with different physical (solubility, optical, etc.) and chemical (adsorption of transition metals and lanthanides, drugs delivery, electrochemical, etc.) properties, differing from the unmodified precursor material. additionally, chitosan provides the possibility to obtain complex systems such as powder, films, fibres, and microspheres.[12–14]

Among various modification processes performed on the chitosan surface (CS), crosslinking can be performed to improve chemical functionalization via a particular functional group. The main crosslinking agents used for this propose are glutaraldehyde, epichlorohydrin, sodium tripolyphosphate, and ethylene glycol diglycidyl ether. Of particular interest is the crosslinking process with epichlorohydrin because its reactions via hydroxyl groups

preserve the NH_2 groups for addition reactions or adsorptions of metal ions.[15,16]

Many studies have demonstrated a large effort to improve the ability of chitosan materials to adsorb metal ions with higher selectivity[17,18], in which the focus was on obtaining new hybrid materials functionalized with aminopolycarboxylates, DTPA, and EDTA derivatives that can be used for the recovery of rare earths, transition metals, and platinum group elements.[19–24] The development of adsorbed trivalent lanthanide ions on chitosan was based on two important goals: First, to obtain a more simple, efficient, low-cost, and environmentally friendly separation methodology; and second, to obtain new hybrid materials that are a combination of the unique properties of chitosan biopolymers and Ln^{3+} ions. It is well known that trivalent lanthanide ions present advantageous spectroscopic properties that are both experimentally and theoretically explored to develop the most promising photonic devices and analytical methods.[25,26] The spectroscopic properties of free lanthanide ions are almost preserved even in compound form. For instance, the intrinsic parity forbidden intra-configurational-$4f^N$ transitions exhibit both low molar absorptivities (10 L mol^{-1} cm^{-1}) and low ligand field splits (~100 cm^{-1}). However, highly photoluminescent materials for practical applications can be only designed via indirect excitation process (e.g. antenna effect). In this case, Ln^{3+} ions are coordinated by organic ligands containing chromophore groups that efficiently absorb and transfer energy to the central metal ion acting as efficient luminescence sensitizers.[27]

Although the noteworthy structural and functional characteristics of chitosan-based materials and the unique spectroscopic properties of Ln^{3+} ions are for practical application, only a few studies have focused on the luminescence properties of an individual material containing these constituents. Most of the studies in this field have dealt with preparation and luminescence properties of CS films doped with lanthanide salts ($LnCl_3$, Ln:Eu and Tb)[28] and the europium complex with thenoyltrifluoroacetone[29], CS containing LaF_3:Eu^{3+}, $NaYF_4$:Yb/Er nanocrystals[30,31] for biological applications, and hybrid materials based on a chitosan core and silica shell.[32] Roosen and Binnemans[33] prepared EDTA- and DTPA-functionalized chitosan biopolymers as stationary phases for adsorption and chromatographic separation of Ln^{3+}, such as Nd^{3+}, Pr^{3+}, and Ho^{3+} from their aqueous mixtures. These novel materials were obtained by homogeneous reactions between the respective dianhydride and commercial CS polymer dissolved in aqueous acetic acid solution. This study proposes, in a different way, the preparation and investigation of the luminescence properties of CS–EDTA–Ln^{3+} materials (in which Ln: Eu^{3+}, Gd^{3+}, and Tb^{3+}) via a heterogeneous synthetic route using precursor and epichlorohydrin crosslinked CS matrices. Furthermore, β-diketonate ligands such as tta, dbm, bzac, and acac were used as luminescence sensitizers to obtain high photoluminescence intensities. Therefore, the role of the crosslinking and antenna effect on the qualitative and quantitative luminescent properties was investigated.

2 | EXPERIMENTAL

2.1 | Materials and methods

Ethylenediaminetetraacetic acid (99%), chitosan (CS) biopolymer of medium molecular weight with a deacetylation amount in the interval of 75–85%, 2-thenoyltrifluoroacetone (tta, 99%), benzoylacetone (bzac, 99%), *N*-methyl-2-pyrrolidone (99%), and epichlorohydrin (ech, 99%) were purchased from Sigma-Aldrich. Sodium bicarbonate, acetic anhydride (99%), and pyridine (99%) were purchased from Vetec. Ethanol and acetone of analytical grade were obtained from Tedia. Acetylacetone (acac, 99.5%) and dibenzoylmethane (dbm, 99% pure) were purchased from Merck. Lanthanide chlorides were prepared from the reactions between the respective oxides (99.99%) and chloride acid (purchased from Sigma-Aldrich) as described.[34] Dianhydride–EDTA was synthesized according to a literature method described by Capretta.[35]

The quantitative analyses of C, H, and N in the CS-functionalized materials were performed by using a Perkin–Elmer model 240 microanalyzer. FT-IR spectra were recorded in KBr pellets in the range 400–4000 cm^{-1} using a Shimadzu spectrophotometer model IRPRESTIGE-21. Europium content on the CS–EDTA material was determined by wavelength dispersive X-ray fluorescence spectroscopy using a EDX-8000) spectrometer (Shimadzu), presenting a Rh anode X-ray tube (50 kV, 28 μA) and silicon drift detector. The data were measuring on the base magnitude of Eu Lα spectral line. Photoluminescence data of the chitosan materials containing lanthanide complexes on their surfaces were recorded at room and liquid nitrogen temperatures by using a Fluorolog-3 spectrofluorometer (Horiba) presenting excitation and emission double-grating monochromators of 0.22 m. The 450 W CW and 50 W pulsed Xe lamps were used as excitation sources, respectively, for steady-state and decay measurements, while a R928P PMT photomultiplier operating at 950 V in the photon-count mode was used as a detector. A cut-off filter of 399 nm was placed between the sample holder and emission monochromator to eliminate second-order diffractions in the photoluminescent spectra.

2.2 | Preparation of CS–EDTA-ln-L and CSech–EDTA-ln-L materials

Crosslinking of CS with epichlorohydrin. About 3 ml of epichlorohydrin (0.038 mol) was added to a suspension of pure chitosan (CS) (6.0 g) of medium molecular weight in an aqueous sodium hydroxide solution (100 ml, 0.001 mol L^{-1}) at 50°C and the reaction system was magnetically stirred for 3 h. The solid product was filtered and washed thoroughly with water and ethanol. Finally, the crosslinked chitosan with epichlorohydrin (CSech) was dried at 60°C under reduced pressure.

EDTA functionalization of CS and CSech. About 6.0 g of CS or its CSech was added to a solution of EDTA dianhydride (4.17 g,

0.016 mol) in N-methyl-2-pyrrolidone (70 ml) at 50°C. The system was magnetically stirred and maintained under nitrogen atmosphere for 24 h. The resulting material was filtered and washed with 60 ml of water and ethanol mixture (50%/50%; v/v). The material was suspended in a sodium bicarbonate aqueous solution (150 ml, 0.1 mol L^{-1}) for 1 h to remove the nonreacted EDTA dianhydride. The CS–EDTA (1) or CSech–EDTA (2) products were filtered, washed with distilled water, and dried at 50°C under reduced pressure.

Ln^{3+} adsorption on CS–EDTA and CSech–EDTA surfaces. Adsorption of Ln^{3+} ions on EDTA-functionalized chitosan (1) and their respective crosslinked EDTA-functionalized chitosan (2) was performed by adding 2.5 g of these chitosan modified matrices in an ethanolic solution containing the lanthanide chloride (0.1 mol L^{-1}) at room temperature, kept under agitation for 24 h. The solids (CS–EDTA–Ln^{3+} and CSech–EDTA–Ln^{3+}) were also filtered, washed thoroughly with water and ethanol, and dried under reduced pressure. At this point, these products were characterized by the presence of water molecules coordinated to the lanthanide ions and, therefore, they were labelled as 1-Ln-H_2O and 2-Ln-H_2O (Ln: Eu^{3+}, Gd^{3+}, or Tb^{3+}) for noncrosslinked and crosslinked chitosan matrices, respectively.

β-diketonate coordination to Ln^{3+} on the CS. 50 ml of ethanolic solution of the β-diketonate ligand (0.01 mol L^{-1} of L: acac, bzac, dbm, or tta) was added to 0.5 g of 1-Ln-H_2O or 2-Ln-H_2O materials. The resulting suspension was stirred at room temperature for 24 h. The solid sample was then filtered and washed thoroughly with water and ethanol, and dried under reduced pressure. These materials were called 1-Ln-L and 2-Ln-L, where L represents the β-diketonate ligands that replace the water molecules in the first coordination sphere of the rare earth ion (Ln: Eu^{3+}, Gd^{3+}, or Tb^{3+}) as illustrated in Figure 1.

3 | RESULTS AND DISCUSSION

3.1 | Characterization of the hybrid materials

Elemental analysis data of the CS, CS–EDTA, CSech, CSech–EDTA, 1-Eu-tta, and 2-Eu-tta systems (Supporting Information Table S1) show an increase in the C/N ratio for the modified surface with epichlorohydrin (CSech) as compared with the CS matrix, indicating an efficient crosslinking process. The introduction of EDTA decreases the C/N ratio for both 1-Ln-L and 2-Ln-L.

Figure S1 shows the FT-IR spectra for CS, CSech, CS–EDTA (1) and CSech–EDTA (2) samples in the interval of 400–4000 cm^{-1}. The spectrum for precursor surface exhibit the characteristic absorption bands of the chitosan skeleton at 3400, 1650, and 1051 cm^{-1} which are attributed to the stretching vibrational modes of the hydroxyl, ν(OH), carbonyl, ν(C=O), remaining N-acetyl, ν(COC), and glucopyranoside rings.[36] CS–EDTA displays a strong absorption band at 1745 cm^{-1} assigned to the asymmetric stretching of the carbonyl groups, ν_s(C=O), from the EDTA moiety covalently connected to the chitosan surface. Spectral data of CSech–EDTA reveal no significant changes compared with that of CS–EDTA sample. Both spectra have the same assignments with no relevant band shifts.

As only Eu–EDTA remains on the CS after washing procedure due to the high coordinating ability of the EDTA unit, the degree of glucosamine–EDTA may be estimated from amount of lanthanide ion adsorbed.[37] The values for Eu^{3+} content determined from wavelength dispersive X-ray fluorescence for the functionalized materials are the following: CS–EDTAEu-H_2O (47.0 mg/g), CS–EDTAEu-dbm (56.0 mg/g) and CS–EDTAEu-tta (50.0 mg/g). The analytical curve is shown in Figure S2. These values indicate that the degree of EDTA functionalization on the CS is around 0.37 mmol/g. It is also

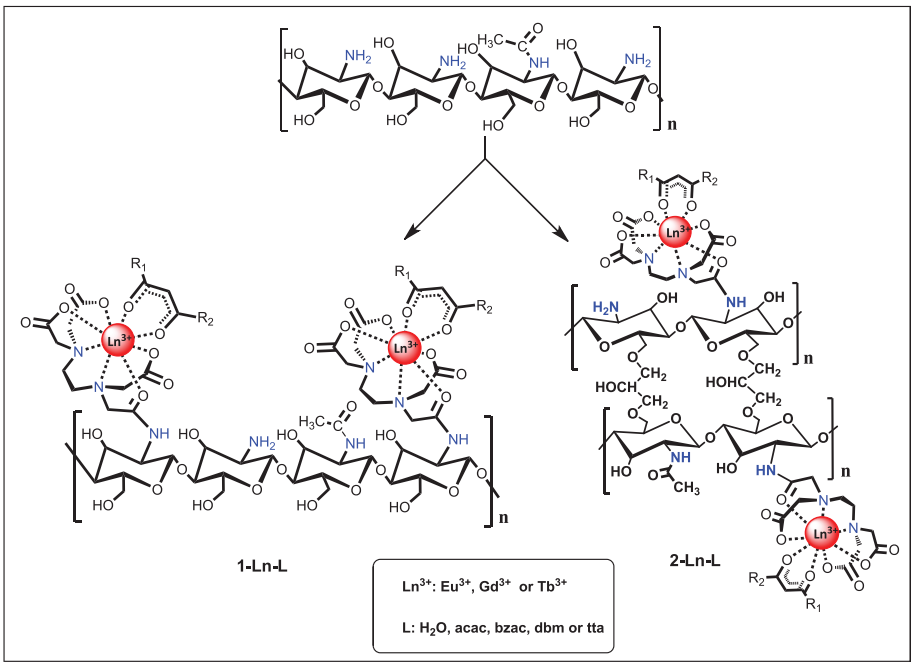

FIGURE 1 Scheme showing proposed structures of the noncrosslinked and crosslinked chitosan surface containing Ln^{3+}–EDTA complexes

interesting to note that the Eu^{3+} content values are very similar to those ones obtained for Binnemans and co-workers.[33]

3.2 | Luminescence properties

3.2.1 | Phosphorescence investigation of the Gd^{3+} hybrid materials

Figure 2 shows the phosphorescence spectra for the hybrid materials 2-Gd-L systems (L: H_2O, acac, bzac, dbm, and tta) were recorded at the liquid nitrogen temperature in the spectral range 410–720 nm with excitation monitored on the intraligand transitions at 350 nm, except for 2-Gd-acac system, when this transition was at 310 nm. Phosphorescence spectra 1-Gd-H_2O (Figure S3) and 2-Gd-H_2O (Figure 2) materials exhibited similar profiles to those of precursor CS matrices (Figure S4)[28], suggesting that chitosan–EDTA did not act as a chromophoric group. Conversely, for the Gd systems containing β-diketonate ligands, new broad emission bands with maxima located at about 460 nm (acac), 490 nm (bzac), 510 nm (dbm), and 530 (tta) were observed (Figure 2). These phosphorescence bands appeared in similar spectral region as in the Tris–diketonate complexes with the same ligands reported by our group[38–40], which were assigned to the phosphorescence from β-diketonate ligands ($T \rightarrow S_0$). It is noteworthy that no significant difference in the spectral profiles between 1-Gd-Land 2-Gd-L materials was observed.

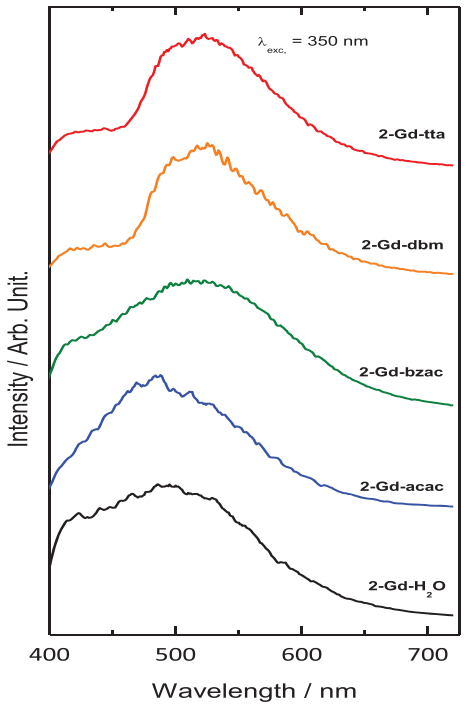

FIGURE 2 Phosphorescence spectra of 2-Gd-L systems (L: H_2O, acac, bzac, dbm, and tta) recorded at 77 K under different excitation wavelengths

3.2.2 | Photoluminescence properties of the Eu^{3+} hybrid materials

The excitation spectra of the samples containing Eu^{3+} complexes (1-Eu-L and 2-Eu-L) covalently linked to the CS were recorded in the spectral range 250–590 nm, with an emission intensity of the hypersensitive $^5D_0 \rightarrow {}^7F_2$ transition around 612 nm (Figure 3, dashed line). In general, these spectra exhibited broad bands between 280 and 550 nm due to absorption of the polymeric CS matrix and β-diketonate ligands. In addition, narrow absorption bands due to Eu^{3+} $4f^6$–$4f^6$ transitions from $^7F_0$ or $^7F_1$ levels to excited $^{2S+1}L_J$ levels were also observed: $^7F_0 \rightarrow {}^5D_1$ (525 nm), $^7F_0 \rightarrow {}^5D_2$ (465 nm), $^7F_0 \rightarrow {}^5L_6$ (394 nm), $^7F_0 \rightarrow {}^5L_7$ (379 nm), and $^7F_1 \rightarrow {}^5D_1$ (535 nm).

The broad absorption band with a maximum at 460 nm in the excitation spectra for 2-Eu-H_2O (Figure 3) and 1-Eu-H_2O (Figure S5) samples could have originated from a small matrix-to-metal energy transfer and by monitoring emission intensities in a spectral region where chitosan matrices also presented significant photoluminescence. However, for 1-Eu-L (Figure S5) and 2-Eu-L (Figure 3) samples (L: acac, bzac, dbm, tta), the highest absorption intensity

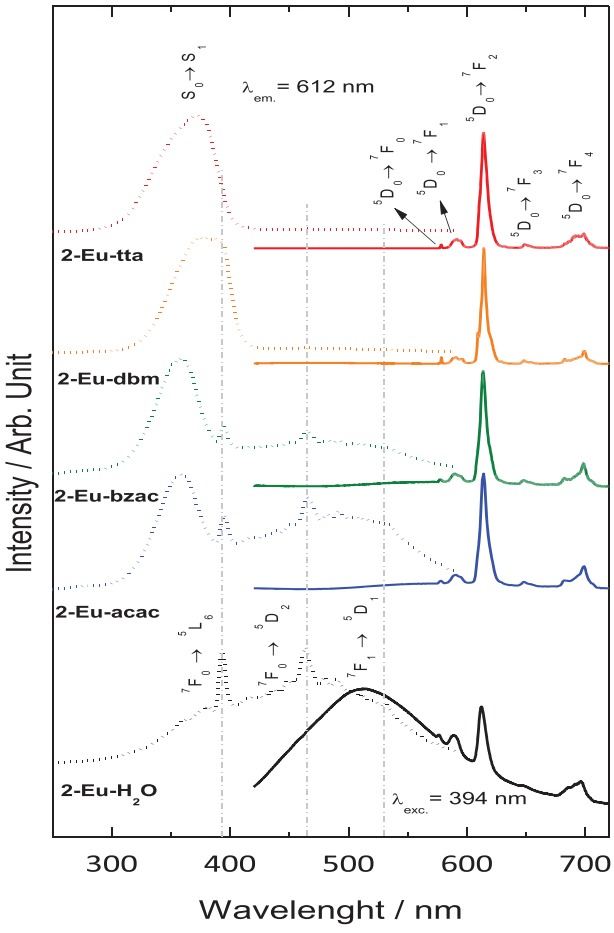

FIGURE 3 Excitation and emission spectra of 2-Eu-L systems (L: H_2O, acac, bzac, dbm, and tta) recorded at room temperature. The excitation spectra were monitored at 612 nm and emission spectra at different excitation wavelengths

bands could be ascribed to the $S_0 \rightarrow S1$ transition centred on β-diketonate ligands. These optical data reflected the high luminescence sensitization of Eu^{3+} ion by these diketonate ligands. It was also observed that the samples containing dbm and tta ligands showed higher relative luminescence intensities of the $S_0 \rightarrow S1$ transition, suggesting that a more operative ligand-to-Eu^{3+} intramolecular energy transfer was taking place.[41]

Upon comparing the excitation spectra between 1-Eu-L and 2-Eu-L matrices, an increase in the relative photoluminescence intensity of the diketonate band was observed for the samples based on crosslinking matrices (2-Eu-L). Because of the crosslinking process, the amine group on the CS became more exposed for an addition reaction with EDTA dianhydride, and the 2-Eu-L system is expected to have a higher number of chelating sites.

Emission spectra of the 2-Eu-L materials were recorded in the spectral range 410–720 nm under excitation on the allowed intraligand transitions ($S_0 \rightarrow S1$) (Figure 3, solid line). The emission spectrum of 2-Eu-H_2O was recorded with direct excitation of the metal ion on the $^7F_0 \rightarrow {}^5L_6$ transition at 394 nm. The 2-Eu-L materials (L: acac, bzac, dbm, tta) exhibited only the characteristic narrow emission bands assigned to the intraconfigurational $^5D_0 \rightarrow {}^7F_J$ (J = 0–4) transitions of the Eu^{3+} ion. Based on these electronic transitions, it was suggested that the chemical environment around Eu^{3+} ion belonged to C_n, C_{nv}, or C_s point groups. In the case of 2-Eu-H_2O water systems, the emission spectra were dominated by the broad emission band attributed to the matrix.

All emission spectra of luminescent materials with different diketonate ligands (Figure 3) showed very similar spectral profiles, suggesting that the chemical environments around Eu^{3+} ions have similar symmetries. In fact, the coordination sphere is generally almost completely saturated by the donor atoms belonging to the aminopolycarboxylate–EDTA ligand. Therefore, when the water molecules were replaced by a diketonate molecule, a minimal perturbation was observed in the chemical environment symmetry around the metal ion. Furthermore, due to the steric hindrance between ligands in the first coordination sphere, only one diketonate ligand was expected to coordinate with the Ln^{3+} ion.

Emission spectra also show a broad band that can be attributed to the emission of the matrix. However, the relative intensity of this band decreased significantly in the following order with the nature of the coordinated ligand: H_2O > acac > bzac > dbm > tta. The lowest relative intensity of this band was observed for the samples containing tta and dbm. This result is in agreement with efficient intramolecular energy transfer processes from diketonate triplet states to the excited of Eu^{3+} ion ($T_1 \rightarrow {}^5D_1$ and $^5D_0$ levels). In addition, there was a significant increase in the relative emission intensities of the $^5D_0 \rightarrow {}^7F_J$ (J = 0–4) transitions of the Eu^{3+} ion from 1-Eu-L (Figure S5) to 2-Eu-L (Figure 3) matrices. This photoluminescence result can be explained based on the increased amount of the Ln^{3+} complexes on the CS due to the crosslinking process.

The spectroscopic properties of the luminescent materials were quantified from the radiative (Arad) and nonradiative decay rates (Anrad), Judd-Ofelt parameters Ω_2, and Ω_4, and emission quantum efficiency. The values of the experimental intensity parameters were calculated from spectral emission data (Figures 3 and S5) according to a published reference.[26] In the present study, the values of the refractive indexes of the samples were taken to be equal to 1.5.

To exclude the emission contribution from the chitosan matrix or organic molecules in the integrated band intensities of the intraconfigurational transitions, all emission spectra were previously corrected considering that these aforementioned parameters were intrinsic to the lanthanide ion. Without this correction, contributions of the matrix and/or ligands in the integrated intensities could provide misleading information on luminescence parameters and chemical environment of the Eu^{3+} ion.

The luminescence decay curves of the 2-Eu-L materials were recorded by monitoring the emission of $^5D_0 \rightarrow {}^7F_2$ transition (612 nm) under excitation in the intraligand $S_0 \rightarrow S_1$ transitions. These data were better adjusted to bi-exponential curves from which $A_{total} = 1/\tau_{av} = (A_1\tau_1 + A_2\tau_2)/(A_1\tau_1^2 + A_2\tau_2^2)$, yielding to the average lifetimes of the $^5D_0$ emitting level, was evaluated.[42,43] Together with the radiative transition rate, obtained by summing the radiative decay rates of all $^5D_0 \rightarrow {}^7F_J$ transitions ($A_{rad} = \Sigma A_{0J}$), the emission quantum efficiency ($\eta = A_{rad}/A_{total}$) and the nonradiative decay rates ($A_{nrad} = A_{total} - A_{rad}$) were determined. Table 1 presents the radiative

TABLE 1 The values of the A_{total}, A_{rad}, and A_{nrad} decay rates, intensity parameters ($\Omega_{\lambda = 2,4}$), and luminescence quantum efficiency (η) of 1-Eu-L and 2-Eu-L materials

Materials	A_{total} (sec^{-1})	A_{rad} (sec^{-1})	A_{nrad} (sec^{-1})	τ_{AV} (10^{-4} sec)	$\Omega_2 \times 10^{-20}$ cm^2	$\Omega_4 \times 10^{-20}$ cm^2	η (%)
1-Eu-H_2O	2235	394	1841	4.47	7.0	8.9	17.6
1-Eu-acac	1657	473	1184	6.03	10.1	8.3	28. 6
1-Eu-bzac	1835	502	1333	5.45	11.3	7.7	27.3
1-Eu-dbm	1813	628	1185	5.52	15.2	8.3	34.7
1-Eu-tta	2073	724	1350	4.82	17.5	9.9	34.9
2-Eu-H_2O	1756	423	1332	5.70	8.0	9.2	24.1
2-Eu-acac	1446	798	648	6.91	19.8	10.3	55.2
2-Eu-bzac	1454	738	716	6.88	18.5	8.9	50.8
2-Eu-dbm	1476	810	666	6.78	19.9	10.8	54.9
2-Eu-tta	1484	867	617	6.74	21.0	12.6	58.4

and nonradiative decay rates, intensity parameters ($\Omega_{\lambda = 2,4}$), and emission quantum efficiency (η) for the 1-Eu-L and 2-Eu-L materials.

The $\Omega_{\lambda = 2,4}$ parameters values changed when the water molecules were substituted by diketonate ligands, suggesting a structural change as these parameters are sensitive to the structure and polarizability around the Eu^{3+} ion (Table 1). Moreover, the substitution of water molecules by diketonate ligands resulted in a significant increase in the A_{rad} values, increasing the relative emission intensity of the hypersensitive $^5D_0 \rightarrow {}^7F_2$ transition. The highest values of the A_{nrad} for the 1-Eu-H_2O and 2-Eu-H_2O systems indicated that the main luminescence quenching process of the Eu^{3+} ions occurred via multiphonon coupling of the ν_s(HOH) and ν_{as}(HOH) vibrational modes with the excited $^5D_0$ emitting level. By introducing the diketonate ligands, the A_{nrad} values were significantly decreased, suggesting efficient displacement of water molecules from the first coordination sphere in the coordinated diketonate ligands.The number of water molecules coordinated to the Eu^{3+} ion (*q*) in these systems was determined using the Horrocks–Supkowski equation, $q = 1.11\ (1/\tau_{H2O} - 1/\tau D2O - 0.31)$[44], where τ_{H2O} and τ_{D2O} are the decay lifetimes of the $^5D_0$ emitting level obtained from the luminescence decay curves for the materials in water and deuterated water suspensions, respectively (Table S2). The value 0.31 in this equation was correlated with the other nonradiative quenching contributions different from OH oscillators.

The calculated values of *q* for the 1-Eu-H_2O and 2-Eu-H_2O systems (Table S2) suggested that two and one water molecules numbers are coordinated to the metal ion, respectively. The *q* values represent the average values considering the inhomogeneity of the chemical environment around the Ln^{3+} ion. For 1-Eu-L and 2-Eu-L materials (L: acac, bzac, dbm, tta), the *q* values were lower than those for the hydrated 1-Eu-H_2O and 2-Eu-H_2O systems, indicating that water molecules in the first coordination sphere of the Eu^{3+} ion were substituted by diketonate ligands. The *q* values were lower for complexes on the crosslinked chitosan with diketonate ligands (rounded to 0.5), suggesting a higher homogeneity in the chemical environment around the metal ion for these systems.

Interestingly, all 2-Eu-L materials presented higher emission quantum efficiency (η) values compared with the similar 1-Eu-L system (Table 1). This result reflected the higher homogeneity of Eu^{3+} sites on the crosslinked chitosan chains.

3.2.3 | Photoluminescence properties of the Tb^{3+} hybrid materials

Figures 4 and S6 show the excitation spectra for the hybrid materials 2-Tb-L and 1-Tb-L systems (L: H_2O, acac, bzac, dbm, and tta), recorded at the interval 250–525 nm, under emission monitored at the $^5D_4 \rightarrow {}^7F_5$ transition (545 nm). These results clearly show a broad absorption band from chitosan matrices [45] with a maximum around 450 nm for all systems. All the excitation spectra also exhibited narrow absorption bands attributed to the $4f^8$ intraconfigurational transitions centred on the Tb^{3+} ion: $^7F_6 \rightarrow {}^5L_9$ (350 nm) and $^7F_6 \rightarrow {}^5D_4$ (488 nm). In addition, a broad absorption band at a longer wavelength was also observed, which is assigned to the $S_0 \rightarrow S_1$ transition centred from β-diketonate ligands. However, higher relative intensities were observed at 310 and 340 nm for 2-Tb-acac and 2-Tb-bzac materials, respectively. It is important to mention that both acac and bzac ligands present their low-lying excited triplet state (T_1) located at energies above the $^5D_4$ emitting levels of the Tb^{3+} ion. These results indicate that acac and bzac ligands act as efficient luminescence sensitizers for Tb^{3+} ion via intramolecular ligand-to-metal energy transfer.

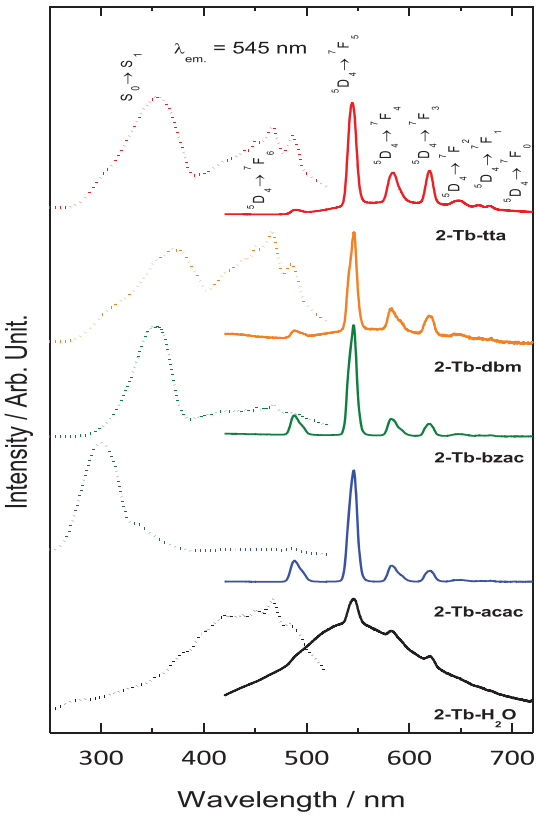

FIGURE 4 Excitation and emission spectra of 2-Tb-L systems (L: H_2O, acac, bzac, dbm, and tta) recorded at room temperature. Excitation spectra were recorded by monitoring the emission intensity of the $^5D_4 \rightarrow {}^7F_5$ transition around 545 nm and emission spectra were recorded with excitation monitored in the intraligand transitions

Emission spectra of hybrid materials 2-Tb-L systems (L: H_2O, acac, bzac, dbm, and tta) were recorded at room temperature in the spectral range 410–720 nm (Figures 4 and S6). All samples were excited at 350 nm, except for ones containing H_2O and acac ligands whose excitation was monitored at 370 and 310 nm, respectively. The emission spectra exhibited characteristic narrow bands due to intraconfigurational-$4f^8$ $^5D_4 \rightarrow {}^7F_J$ transitions (J = 6, 5, 4, 3, 2, 1 and 0) centred on the Tb^{3+} ion. Furthermore, a broad emission band due to the polymer matrices was also observed. However, the relative intensities of the $4f^8$–$4f^8$ transitions for both 1-Tb-L and 2-Tb-L materials increased significantly, following the trend: H_2O < tta ~ dbm < bzac < acac, and showing an inverse luminescence trend for those with Eu^{3+} ion. This spectroscopic behaviour is associated with change in the relative position of the low-lying triplet states (T_1) of the diketonate

ligands and the $^5D_0$ and $^5D_4$ emitting levels of the Eu^{3+} and Tb^{3+} ions, respectively. However, it is to be noted that acac and bzac are better luminescence sensitizers for Tb^{3+} ion than for Eu^{3+} ion, leading to highly bright green-emitting materials.

3.2.4 | Luminescence colour of Ln^{3+} materials

To determine the colour emitted by the hybrid materials, the CIE coordinates (x,y) colours were calculated from the emission spectra data by using the program SPECTRALUX developed by Santa-Cruz[46] (Table S3). The numerical values of the colour coordinates were located in the regions around red and green, respectively (Figures 5 and S7). The presence of different emitting species in the same material (Ln^{3+}, polymeric matrices and/or ligands) contributed significantly to the multicolour-tuneable luminescence. The emitted colour was largely depending on the ratio among the relative emission intensity bands. The purest red luminescence colour was assigned to 1-Eu-tta and 2-Eu-tta (Figure S8) with the CIE coordinates (x,y) colour (0.64, 0.32) and (0.69, 0.31), respectively, reflecting the most operative tta→Eu^{3+} intramolecular energy transfer in these materials (Figure 5). Conversely, 1-Tb-acac and 2-Tb-acac exhibited colour coordinates closest to the green region. Furthermore, crosslinking-based chitosan materials exhibited more localized coordinate colours in the CIE diagram compared with noncrosslinked materials, indicating the presence of a broad emission band from chitosan matrices. It is noteworthy that, due to the significant emission from chitosan matrices, europium hydrated systems presented a coordinate colour close to the white emission colour (Figure 5).

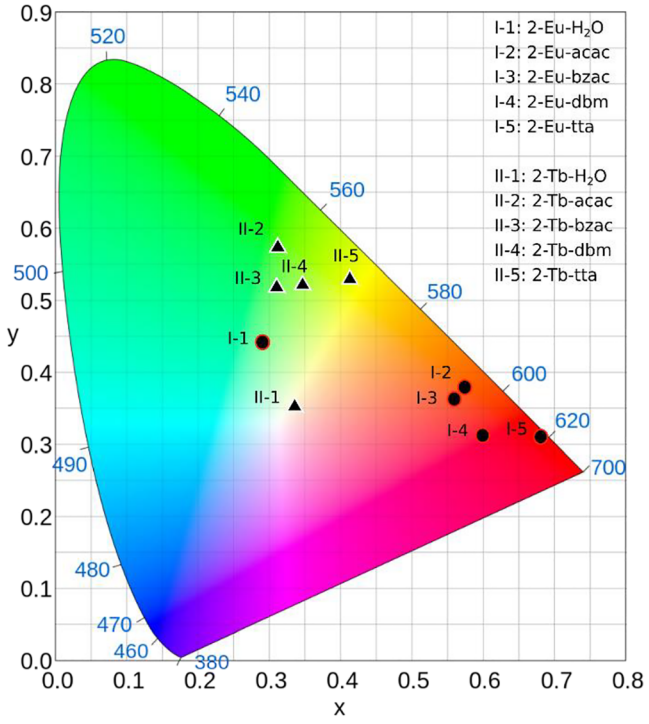

FIGURE 5 Commission Internationale de l'Eclairage (CIE) chromaticity diagram presenting (x,y) colour coordinates for 2-Eu-L and 2-Tb-L (L: H_2O, acac, bzac, dbm, and tta)

4 | CONCLUSION

New types of materials 1-Ln-L and 2-Ln-L containing EDTA–Ln–L (in which Ln^{3+}: Eu^{3+}, Gd^{3+}, and Tb^{3+}; and L: H_2O, tta, dbm, bzac, and acac) complexes covalently bonded to the precursor and crosslinked with epichlorohydrin CSs were prepared. The preparation method led to luminescent materials based on the chitosan biopolymer containing lanthanide ions combined with diketonate ligands. Crosslinking showed an important role in luminescence properties of the materials. The success of the EDTA moiety covalently linked and ready to chelate resulted in hybrid materials with up to ~58% emission quantum efficiency. Concerning this aspect, it was found that the crosslinking process played an important role in the luminescence properties of the final material, increasing the radiative rate and providing lower nonradiative rate values. Nonetheless, among all organic ligands studied, some of these were able to sensitize better than others for a particular ion (tta for Eu^{3+} and acac and bzac for Tb^{3+}), mainly due to the best position of the triplet state of these ligands with respect to the emitting level of Eu^{3+} and Tb^{3+} ions. The colour coordinates of the complexes containing the Eu^{3+} and Tb^{3+} ions were located in the regions around the red and green, respectively. However, the EDTA–Eu–tta complex presented coordinates with more pure colour, whereas the systems containing EDTA–Tb–acac presented as pure green. This trend in the Eu^{3+} and Tb^{3+} systems is the result of more efficient sensitization of tta ligands to the Eu^{3+} ion, while the acac and bzac ligands acted as efficient sensitizers for the Tb^{3+} ion. Although this study was concerned with photoluminescence properties of Eu^{3+} and Tb^{3+} hybrid materials, in which the luminescence of lanthanide ions is sensitized by ligands, intramolecular ligand-to-metal energy transfer can also be observed for other lanthanide ions in similar systems. Ethylenediaminetetraacetic acid (EDTA)-functionalized chitosan containing lanthanide ions could be used as fluorescence sensor for biological molecules and metal ions in aqueous solutions.

ACKNOWLEDGEMENTS

We thank CAPES (Coordenação de Aperfeiçoamento de Pessoal de Nível Superior), CNPq (Conselho Nacional de Desenvolvimento Científico e Tecnológico), FAPESP (Fundação de Amparo à Pesquisa do Estado de São Paulo), and FINEP (Empresa Brasileira de Inovação e Pesquisa) for financing this research.

ORCID

Israel F. Costa https://orcid.org/0000-0002-4829-0663
Ercules E.S. Teotonio https://orcid.org/0000-0003-0184-0645

REFERENCES

[1] Z. Shariatinia, *Adv. Colloid Interface Sci.* **2019**, *263*, 131.

[2] R. J. B. Pinto, L. D. Carlos, P. A. A. P. Marques, A. J. D. Silvestre, C. S. R. Freire, *J. Appl. Polym. Sci.* **2014**, *131*, 41169.
[3] M. N. V. R. Kumar, R. A. A. Muzzarelli, C. Muzzarelli, H. Sashiwa, A. J. Domb, *Chem. Rev.* **2004**, *104*, 6017.
[4] W. Suginta, P. Khunkaewla, A. Schulte, *Chem. Rev.* **2013**, *113*, 5458.
[5] C. Zheng, Y. Mi, *X. Zheng. Luminescence.* **2018**, *33*, 399.
[6] E. Guibal, *Prog. Polym. Sci.* **2005**, *30*, 71.
[7] N. Ahmed, S. Tarannum, Z. N. Siddiqui, *RSC Adv.* **2015**, *5*, 50691.
[8] M. Zhang, W. Dai, M. Yan, S. Ge, J. Yu, X. Song, W. Xu, *Analyst* **2012**, *137*, 2112.
[9] F. Ding, H. Deng, Y. Du, X. Shi, Q. Wang, *Nanoscale* **2014**, *6*, 9477.
[10] M. Rinaudo, *Prog. Polym. Sci.* **2006**, *31*, 603.
[11] V. K. Mourya, N. N. Inamdar, *React. Funct. Polym.* **2008**, *68*, 1013.
[12] M. N. V. Ravi Kumar, *React. Funct. Polym.* **2000**, *46*, 1.
[13] H. Sashiwa, S. Aiba, *Prog. Polym. Sci.* **2004**, *29*, 887.
[14] A. El Kadib, M. Bousmina, *Chem. – Eur. J.* **2012**, *18*, 8264.
[15] W. S. W. Ngah, S. Ab Ghani, A. Kamari, *Bioresour. Technol.* **2005**, *96*, 443.
[16] A.-H. Chen, S.-C. Liu, C.-Y. Chen, C.-Y. Chen, *J. Hazard. Mater.* **2008**, *154*, 184.
[17] I. M. N. Vold, K. M. Vårum, E. Guibal, O. Smidsrød, *Carbohydr. Polym.* **2003**, *54*, 471.
[18] S. Babel, *J. Hazard. Mater.* **2003**, *97*, 219.
[19] E. Repo, J. K. Warchoł, A. Bhatnagar, M. Sillanpää, *J. Colloid Interface Sci.* **2011**, *358*, 261.
[20] C. Mack, B. Wilhelmi, J. R. Duncan, J. E. Burgess, *Biotechnol. Adv.* **2007**, *25*, 264.
[21] K. Inoue, T. Yamaguchi, M. Iwasaki, K. Ohto, K. Yoshizuka, *Sep. Sci. Technol.* **1995**, *30*, 2477.
[22] E. Repo, J. K. Warchoł, T. A. Kurniawan, M. E. T. Sillanpää, *Chem. Eng. J.* **2010**, *161*, 73.
[23] F. Zhao, E. Repo, D. Yin, L. Chen, S. Kalliola, J. Tang, E. Iakovleva, K. C. Tam, M. Sillanpää, *Sci. Rep.* **2017**, *7*, 15811.
[24] Y. Wang, A. Pitto-Barry, A. Habtemariam, I. Romero-Canelon, P. J. Sadler, N. P. E. Barry, *Inorg. Chem. Front.* **2016**, *3*, 1058.
[25] J. -C. G. Bünzli, *Acc. Chem. Res.* **2006**, *39*, 53.
[26] G. de Sá, O. Malta, C. de Mello Donegá, A. Simas, R. Longo, P. Santa-Cruz, E. da Silva, *Coord. Chem. Rev.* **2000**, *196*, 165.
[27] G. Bottaro, F. Rizzo, M. Cavazzini, L. Armelao, S. Quici, *Chem. – Eur. J.* **2014**, *20*, 4598.
[28] R. S. Oliveira, D. O. Maia, M. R. Pereira, F. R. G. E Silva, *J. Macromol. Sci. Part a* **2010**, *47*, 392.
[29] M. Tsvirko, E. Mandowska, M. Biernacka, S. Tkaczyk, A. Mandowski, *J. Lumin.* **2013**, *143*, 128.
[30] F. Wang, Y. Zhang, X. Fan, M. Wang, *Nanotechnology* **2006**, *17*, 1527.
[31] Q. Chen, X. Wang, F. Chen, Q. Zhang, B. Dong, H. Yang, G. Liu, Y. Zhu, *J. Mater. Chem.* **2011**, *21*, 7661.
[32] F. Liu, L. D. Carlos, R. A. S. Ferreira, J. Rocha, M. C. Ferro, A. Tourrette, F. Quignard, M. Robitzer, *J. Phys. Chem. B* **2010**, *114*, 77.
[33] J. Roosen, K. Binnemans, *J. Mater. Chem. A* **2014**, *2*, 1530.
[34] G. P. Pires, I. F. Costa, H. F. Brito, W. M. Faustino, E. E. S. Teotonio, *Dalton Trans.* **2016**, *45*, 10960.
[35] A. Capretta, R. B. Maharajh, R. A. Bell, *Carbohydr. Res.* **1995**, *267*, 49.
[36] D. de Britto, S. P. Campana-Filho, *Thermochim. Acta* **2007**, *465*, 73.
[37] M. Donmez, H. A. Oktem, M. D. Yilmaz, *Carbohydr. Polym.* **2018**, *180*, 226.
[38] H. F. Brito, O. L. Malta, M. C. F. C. Felinto, E. E. S. Teotonio (Eds), Luminescence Phenomena Involving Metal Enolates, in *Z. Rappoport, PATAIS Chem. Funct. Groups*, John Wiley& Sons, Chichester **2010**.
[39] F. A. Silva Jr., H. A. Nascimento, D. K. S. Pereira, E. E. S. Teotonio, H. F. Brito, M. C. F. C. Felinto, J. G. P. Espínola, G. F. Sá, W. M. Faustino, *J. Braz. Chem. Soc.* **2013**, *24*, 601.
[40] E. E. S. Teotonio, H. F. Brito, G. F. de Sá, M. C. F. C. Felinto, R. H. A. Santos, R. M. Fuquen, I. F. Costa, A. R. Kennedy, D. Gilmore, W. M. Faustino, *Polyhedron* **2012**, *38*, 58.
[41] K. Binnemans, *Coord. Chem. Rev.* **2015**, *295*, 1.
[42] W. T. Carnall, H. Crosswhite, H. M. Crosswhite, Energy level structure and transition probabilities in the spectra of the trivalent lanthanides in LaF_3, Argonne National Lab.(ANL), Argonne **1978**.
[43] H. Wang, Y. Ma, H. Tian, N. Tang, W. Liu, Q. Wang, Y. Tang, *Dalton Trans.* **2010**, *39*, 7485.
[44] R. M. Supkowski, W. D. Horrocks Jr., *Inorg. Chim. Acta* **2002**, *340*, 44.
[45] J. Xue-yin, J. Yan, Z. Zhi-lin, X. Shao-hong, *J. Cryst. Growth* **1998**, *191*, 692.
[46] P. A. Santa-Cruz, and F.S. Teles, *Spectra Lux Software v. 2.0. Ponto Quântico Nanodispositivos/RENAMI*, Recife 2003.

SUPPORTING INFORMATION

Additional supporting information may be found online in the Supporting Information section at the end of this article.

How to cite this article: Costa IF, Pires GP, Espínola JGP, et al. Luminescence properties of the Ln–EDTA complexes covalently linked to the chitosan biopolymers containing β-diketonate as antenna ligands. *Luminescence*. 2020;35:365–372. https://doi.org/10.1002/bio.3735